A kinetic model for the pattern and amounts of hydrate precipitated from a gas steam: Application to the Bush Hill vent site, Green Canyon Block 185, Gulf of Mexico

Duo Fu Chen,[1,2] and Lawrence M. Cathles III[1]

Received 10 October 2001; revised 10 March 2002; accepted 18 July 2002; published 30 January 2003.

[1] We construct a linear kinetic model of hydrate crystallization from a gas stream. We use this model to predict the fraction of gas that crystallizes as hydrate in the subsurface of Bush Hill, and the depth profile of subsurface hydrate accumulation. This is possible because the Bush Hill vent is fed by reservoir gas from the nearby Jolliet field whose composition is known. On the average, ~9% of the vent gas is precipitated as hydrate in the subsurface. Although other explanations are possible, the observed vent gas compositions and the greater range of hydrate gas compositions are consistent with a single source gas whose venting rate varies by a factor of at least 3 over periods of a few years or less. The predicted depth profile of hydrate accumulation and the hydrate content of the Bush Hill mound suggest that between $\sim 1.1 \times 10^9$ and 2.8×10^9 m^3 (STP) of gas may have accumulated as hydrate between the seafloor and ~614-m depth. For the radiometrically and geologically suggested system age of 10,000 years, the time average venting rate is $\sim 10^6$ m^3/yr (0.7×10^6 kg/yr). If distributed evenly across the 600 m diameter mound, as suggested by echo sounder images, the methane flux is >3.2 kg/m^2 yr. This is $>10^3$ times that inferred for hydrates associated with bottom-simulating seismic reflectors. The subsurface hydrate accumulation and the cumulative methane venting are related. We show how both may be estimated from measurements of vent gas composition, bottom water temperature, and geothermal gradient. *INDEX TERMS:* 1055 Geochemistry: Organic geochemistry; 4820 Oceanography: Biological and Chemical: Gases; 4825 Oceanography: Biological and Chemical: Geochemistry; 4842 Oceanography: Biological and Chemical: Modeling; 9350 Information Related to Geographic Region: North America; *KEYWORDS:* hydrate, resource, venting, hydrocarbon, gas, kinetic

Citation: Chen, D. F., and L. M. Cathles III, A kinetic model for the pattern and amounts of hydrate precipitated from a gas steam: Application to the Bush Hill vent site, Green Canyon Block 185, Gulf of Mexico, *J. Geophys. Res.*, *108*(B1), 2058, doi:10.1029/2001JB001597, 2003.

1. Introduction

[2] Gas hydrate is an ice-like crystalline mineral in which a rigid cage of water molecules encloses hydrocarbon and nonhydrocarbon gas molecules [*Sloan*, 1998]. Natural gas hydrates occur worldwide in polar regions and in subthermocline oceanic environments, especially in areas of onshore and offshore permafrost and in sediments on continental margin slopes [*Kvenvolden*, 1998]. The structure of the hydrate determines the gas molecules contained. Methane, and to an extent ethane, are the main hydrocarbons found in Structure I hydrate. Structure II hydrates typically encage methane through butane, and sometimes encage carbon dioxide and nitrogen. Heavier hydrocarbon molecules such as isopentane are the guest molecules in Structure H hydrate [*Sloan*, 1998; *Sassen and MacDonald*, 1994]. Structure I hydrate generally contains methane produced via bacterial reduction of CO_2 in shallow sediments at low temperatures [*Kvenvolden*, 1998; *Sassen et al.*, 1999b]. Structure II and H hydrates mainly contain thermogenic hydrocarbon gases, and these hydrates are usually associated with thermogenic gas seeps [*Sassen and MacDonald*, 1994; *Ginsburg and Soloviev*, 1997, 1998; *Collett*, 1993].

[3] The Gulf of Mexico is a classic area of gas hydrate occurrence. Hydrates have been sampled at 50 sites where the water depth exceeds ~440 m [*Kennicutt et al.*, 1985; *MacDonald et al.*, 1994; *Sassen and MacDonald*, 1994; *Kvenvolden*, 1995; *Booth et al.*, 1996; *Sassen et al.*, 2001a, 2001b] and all three hydrate structures have been found. Huge amounts of methane may be trapped as hydrate in the Gulf. *Collett* [1995] and *Collett and Kuuskraa* [1998] estimate there is $\sim 0.89 \times 10^{14}$ m^3 of gas trapped as hydrate in the Gulf of Mexico. In a more detailed analysis, *Milkov and Sassen* [2001] estimate $10-14 \times 10^{12}$ m^3 of hydrate gas in the northwestern Gulf of Mexico, and suggest that

[1]Department of Geological Sciences, Cornell University, Ithaca, New York, USA.
[2]Guangzhou Institute of Geochemistry, Chinese Academy of Sciences, Guangzhou, China.

0148-0227/03/2001JB001597$09.00

~80% is in faults at the margins of salt withdrawal minibasins where thermogenic gas has vented.

[4] Thermogenic seeps are in fact almost always associated with faults. Oil-related hydrocarbon gases migrate through these faults from deeply buried petroleum source rocks and reservoirs [*Kornacki et al.*, 1994; *Wenger et al.*, 1994; *Sassen et al.*, 1998, 2001a, 2001b]. The gas is usually primarily thermogenic [*Sassen et al.*, 1998, 1999a, 2000, 2001b]. Bacterial methane gas or gas from bacterial hydrocarbon oxidation is sometimes present [*Sassen et al.*, 1998, 1999a, 2000, 2001b; *Sassen and MacDonald*, 1994, 1997]. Gases from hydrate decomposition could be present [*Roberts*, 2001; *MacDonald et al.*, 1994], but this seems to be limited to the outer few meters of exposed hydrate mounds [*Milkov et al.*, 2000].

[5] The faults that vent thermogenic hydrocarbons are commonly located at the rims of salt withdrawal minibasins [*Sassen et al.*, 1999b, 2001a]. Salt migration strongly influenced the structural style of the basin when Tertiary siliclastic sediments deposited on the ~2-km-thick Louann salt. Basins formed when this loading caused salt to withdraw into adjacent diapers. Faults on these margins are particularly favorable vent sites. Vents have been found in all stages of development. In the most active vents, gas plumes extend from the vents to the sea surface. Complex chemosynthetic communities and authigenic carbonate rock (as well as gas venting and hydrate accumulation) mark the sites of venting [*Brooks et al.*, 1984, 1986; *Kennicutt et al.*, 1988; *Roberts and Aharon*, 1994; *Roberts*, 1996, 2001; *Roberts and Carney*, 1997; *Roberts*, 2001; *Sassen et al.*, 2001a]. Hydrates accumulated in faults could extend to the base of the hydrate stability field at >1 km below the ocean floor [*Milkov and Sassen*, 2000] and thus volumes of hydrate sufficient to represent gas resources could accumulate.

[6] The mix of gases trapped in thermogenic hydrocarbon hydrates provides information on the physical and chemical conditions that existed during their crystallization which is not available in the biogenic, structure I hydrates that contain only methane [*Sloan*, 1998; *Sassen et al.*, 1999a, 2000, 2001a, 2001b]. This is because the abundance of ethane, propane and isobutane will decrease relative to methane as Structure II hydrates crystallize from thermogenic gas. Hydrate has a greater affinity for the heavier gases. Still heavier molecules (e.g., isopentane) are not affected because their diameter is too large to fit within Structure II hydrate cages [*Sloan*, 1998; *Sassen et al.*, 2000, 2001b]. The result is that the composition of vent gases can tell us how much hydrate has precipitated in the subsurface.

[7] The hydrates and associated vent gases at the Bush Hill site in Green Canyon Block 185 offer a natural laboratory to study how hydrate precipitation affects gas composition because (1) Bush Hill is a site of rapid and ongoing gas venting [*Roberts and Aharon*, 1994; *Sassen et al.*, 1993, 1999a; *Sassen and McDonald*, 1994; *MacDonald et al.*, 1994, 2000; *Roberts*, 2001], (2) the gases at Bush Hill derive from the same source as gasses in the nearby Jolliet gas reservoirs, and (3) abundant data are available on the Jolliet reservoir gases, the Bush Hill vent gases and the Bush Hill hydrates.

[8] The spatial relationship of the Bush Hill vent to the Jolliet oil and gas fields is shown in Figure 1. Gas hydrate accumulations and chemosynthetic communities are present

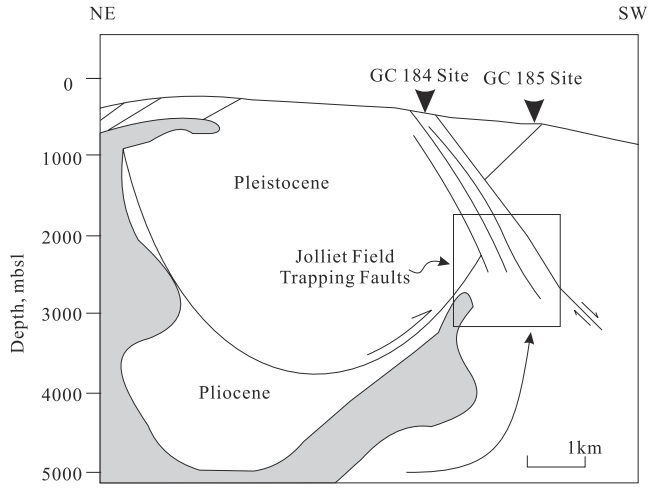

Figure 1. NE to SW cross section showing the location of the Jolliet gas reservoirs, the normal faults that localize them and cut the surface in Green Canyon Block 184, and the antithetic fault that connects this system to the Green Canyon Block 185 Bush Hill vent site. Arrow indicates hypothesized gas migration filling the reservoirs and feeding the surface vents. Reported by *Sassen and McDonald* [1994, 1997] and *Sassen et al.* [1998, 1999a, 1999b].

at two sites as indicated by arrows. The location of the Jolliet oil and gas reservoirs is indicated by the box in the figure. The major growth fault system that contains the Jolliet hydrocarbon reservoirs intersects the seafloor at the active site of hydrocarbon discharge that lies in GC 184 [*Brooks et al.*, 1984, 1986]. The Bush Hill vent site in GC 185 receives hydrocarbon gas from a fault that is antithetic to the growth faults that trap Jolliet the oil and gas reservoirs [*Sassen et al.*, 2001a].

[9] Present-day gas venting at Bush Hill produces a plume that is dramatically visible on echo sounder records. In August of 2000 the echo sounder plume originated from a 600 m interval at the seafloor centered on Bush Hill and nearly reached the surface. Gas bubbles 2 to 3 cm in diameter were breaching the sea surface over the site, leaving oil slicks as they dissipated. The composition of the vent gas at Bush Hill is consistent with stripping of C_{2+} hydrate-forming gases by hydrate precipitation. Since there is no isotopic fractionation during hydrate precipitation, the isotopic similarity of the Jolliet reservoir gases, the vent gases, and the Bush Hill hydrates is very strong evidence that all the gasses are from a common source [*Roberts*, 2001; *Sassen et al.*, 2001a].

[10] Two features of the Bush Hill vent are particularly important for this paper. First gases are actively and continuously venting at the present time. The venting gas is not all precipitated as hydrate in the subsurface. It could all be precipitated because the shallow subsurface is within the stability field of Structure II methane hydrate. The gas venting must therefore be rapid enough, relative to the rate of hydrate formation, that hydrate precipitation is kinetically inhibited and free gas can reach the surface. Second, the sampled range in hydrate gas compositions is much larger than that of the sampled vent gas compositions.

Table 1. Compositions of Jolliet Reservoir Gas, Bush Hill Vent Gas, and Bush Hill Structure II Hydrate Gas[a]

	C_1	C_2	C_3	i-C_4	n-C_4	C_{3+4}
			Jolliet Reservoir Gas			
J-1	90.5	6.0	2.3	0.3	0.6	3.2
J-2	90.2	6.5	2.3	0.3	0.5	3.1
J-3	86.2	8.3	3.8	0.5	0.9	5.2
J-4	87.1	7.5	3.5	0.5	0.9	4.9
J-5	87.8	7.1	3.3	0.5	0.9	4.7
J-6	87.0	7.7	3.4	0.5	0.9	4.8
J-7	87.4	6.9	3.5	0.6	1.1	5.2
J-8	91.4	5.1	2.4	0.4	0.6	3.4
J-9	87.3	7.4	3.4	0.5	0.9	4.8
J-10	88.1	7.3	3.1	0.5	0.8	4.4
J-11	84.6	8.9	4.1	0.7	1.2	6.0
J-12	89.8	5.5	2.8	0.5	0.9	4.2
J-13	85.7	8.4	3.7	0.6	1.0	5.3
J-14	86.6	7.3	3.8	0.6	1.1	5.5
J-15	87.3	7.4	3.7	0.5	0.7	4.9
J-16	86.5	7.8	3.6	0.6	1.0	5.2
Mean	87.7	7.2	3.3	0.5	0.9	4.675
			Vent Gas			
V-1	93.2	4.3	1.5	0.3	0.6	2.40
V-2	93.5	4.3	1.4	0.2	0.4	2.00
V-3	94.7	3.9	0.7	0.1	0.5	1.30
V-4	94.6	3.8	0.7	0.1	0.5	1.30
V-5	91.1	4.8	1.8	0.4	1.2	3.40
V-6	90.4	4.5	3.7	0.6	0.6	4.90
V-7	95.9	2.4	1.2	<0.1	0.3	1.50
V-8	93.4	4.1	1.5	0.3	0.5	2.30
Mean	93.4	4.0	1.6	0.3	0.6	2.39
			Hydrate Gas			
H-1	83.1	7.6	8.1	0.9	0.2	9.20
H-2	71.7	10.6	12.6	2.6	1.7	16.90
H-3	80.2	9.4	7.3	1.6	1.2	10.10
H-4	72.1	12.4	11.4	2.3	1.6	15.30
H-5	85.7	6.3	6.1	1.1	0.8	8.00
H-6	71.8	3.4	18.8	5.7	0.3	24.80
H-7	73.9	4.9	16.3	4.6	0.2	21.10
H-8	72.1	10.5	12.4	2.5	1.7	16.60
Mean	76.3	8.1	11.6	2.7	1.0	15.25

[a]Values are in wt %. Jolliet reservoir gas, J-1 through J-16; Bush Hill vent gas, V-1 through V-8; Bush Hill Structure II hydrate gas, H-1 through H-8. Reported by *Sassen and MacDonald* [1997, 1994] and *Sassen et al.* [1998, 1999a, 1999b].

[11] The objective of this paper is to construct a kinetic model of gas venting and hydrate precipitation at the Bush Hill vent and calibrate it to the observed vent, hydrate, and reservoir compositions. The model we construct is for the situation of kinetically controlled crystallization where a free gas is present throughout. We show that such a model, while quite different from other published hydrate accumulation models where no free gas is present in the hydrate stability zone [e.g., *Xu and Ruppel*, 1999], can explain the observations at the Bush Hill site.

2. Development of a Kinetic Model for Hydrate Precipitation at Bush Hill

2.1. Vent Gases and Hydrates at Bush Hill

[12] All available hydrate and vent gas analyses from the literature from the Bush Hill vent site, and all available analyses of Jolliet reservoir gas are listed in Table 1. The mean and range of this compositional data are plotted in Figure 2. Methane is the main component in all three types of gas. Its mass fraction is highest in vent gas (mean 93 wt %, n = 11) and lowest in hydrate gas (mean 75 wt %, n = 12). Conversely, the relative abundance of C_2 and C_{3+4} is highest in the hydrate gas (8.9 wt % and 15.1 wt % respectively) and lowest in vent gas (3.9 wt % and 2.6 wt % respectively). The methane, C_2, and C_{3+4} compositions of the Jolliet gas are intermediate between the vent and hydrate compositions. The shift in vent and hydrate gas composition from Jolliet reservoir composition is largest for C_{3+4} and smallest for C_1. These, as well as isotopic relationships, indicate that the vent gas at the Bush Hill vent in GC 185 are Jolliet reservoir gases that have been shifted in composition by hydrate precipitation [*Sassen et al.*, 1999a, 2001a].

2.2. Chemical Disequilibrium of Vent Gases

[13] Gas hydrate stability is a function of pressure (depth below the sea surface), temperature, free gas composition, water gas saturation, and water salinity [*Sloan*, 1998; *Miles* 1995; *Milkov and Sassen*, 2000]. The stability model we construct for Jolliet gases as a function of temperature, pressure, and gas composition is shown in Figure 3. Figure 3 plots the hydrate equilibrium pressure for feed gases with the composition of the Jolliet reservoir analyses at temperatures between 5° and 23°C. The equilibrium pressures at which these gases are in equilibrium with Structure II hydrate are calculated using the CSMHYD computer program of *Sloan* [1998] for a pore water salinity of 3.54 wt % NaCl, which is the normal deepwater salinity in the Gulf of Mexico [*Fu and Aharon*, 1998]. The composition of the 16 Jolliet Reservoir gases is represented in Figure 3 by the weight percent $C_{3+4}^{J\text{-}gas}$ in these gases, but the measured C_1 through C_4 compositions were used in the calculations. Because we wish the figure to apply generally the axis is labeled as vent gas; the Jolliet gases are treated as a special instance of vent gas.

[14] Figure 3 shows that the Jolliet gas data form linear trends at each temperature. Regressions of these trends shows the data can be fit with an R^2 = 0.94 by a linear

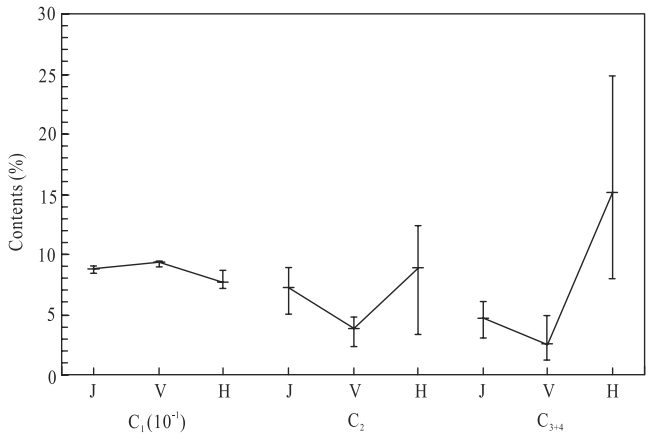

Figure 2. Weight percent C_1, C_2, and C_{3+4} composition of Jolliet reservoir gas (J), vent gas (V), and hydrate gas (H) at Bush Hill, Green Canyon Block 185. The mean values are indicated by the middle bar, and the data range by the upper and lower bars. Data are from Table 1.

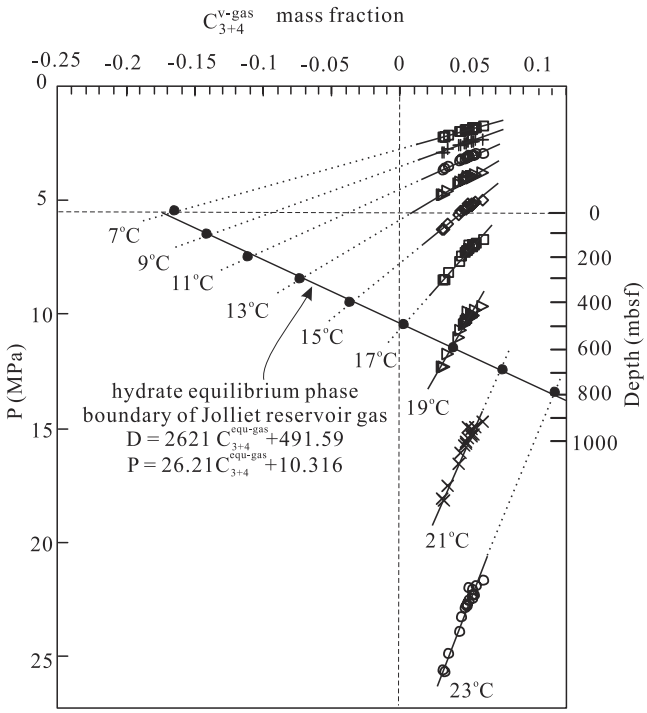

Figure 3. Pressures at which all Jolliet reservoir gases first precipitate hydrate are calculated for 3.54 wt % NaCl pore waters and plotted as a function of their C_{3+4} mass fractions for temperatures ranging from 23° to 5°C (circle through triangle symbols). Regressions through this data are extrapolated to the hydrostatic pressure-temperature profile below Bush Hill (solid line with solid circle). To the right of the vertical dotted line, this solid line represents the equilibrium hydrate phase boundary; to the left it provides a measure of the thermodynamic disequilibrium of positive $C_{3+4}^{v\text{-}gas}$ compositions.

equation whose coefficients are third order polynomials in temperature:

$$P = aC_{3+4}^{J-gas} + b \tag{1}$$

$$a = -10.44 + 0.2712T - 0.0439T^2 - 0.0106T^3 \left(R^2 = 0.9931\right)$$

$$b = 0.2969 + 0.8305T - 0.1032T^2 + 0.0054T^3 \left(R^2 = 0.9989\right)$$

In this equation, T is the temperature in °C (valid between 1°C and 23°C), P is the pressure in MPa, and $C_{3+4}^{J\text{-}gas}$ is the $C_3 + C_4$ mass fraction of Jolliet reservoir gas.

[15] The geothermal gradient is well defined by bottom hole temperature measurements made in the Jolliet reservoirs. Based on 18 temperature measurements by *Bascle et. al.* [2001] and 19 measurements provided by Conoco, the gradient is 20.1°C/km. The pore fluid pressure is hydrostatic to depths of ~1400 m (Conoco site geologist, personal communication, 2001). The geothermal gradient can be affected by rapid vertical fluid flow [*Roberts*, 2001; *Roberts and Carney*, 1997], but we do not consider this possibility in this paper. For water salinities of 3.54 wt % and a geothermal gradient of 20°C/km, the hydrostatic pressure gradient is very close to 0.01 MPa/m. The water depth at the Bush Hill vent is 540 m. Measured bottom water temperature in GC 185 is 6–11°C with a mean 7°C [*MacDonald et al.*, 1994; *Sassen and MacDonald*, 1994]. Seafloor temperature is affected by loop current eddies spinning off from the Gulf Stream [*Roberts*, 2001; *MacDonald et al.*, 1994, 2000; *Roberts and Carney*, 1997]. In our calculations we choose a constant bottom water temperature of 7°C. Temperature and pressure are then related to depth below the seafloor:

$$P = 5.4 + 0.5(T - 7), \tag{2}$$

where T is temperature in °C and P is pressure in MPa.

[16] Using (2), each regression line in Figure 3 can be projected to the pressure (or depth below the seafloor) at which its temperature would occur. The solid line in Figure 3 shows the locus of these points and represents the hydrate stability boundary in the subsurface at Bush Hill as a function of the C_{3+4} mass fraction of feed gas. This hydrate stability line in Figure 3 can be described by either of the following equations:

$$\begin{aligned} C_{3+4}^{equ} &= \frac{P}{26.2} - 0.3936 \\ C_{3+4}^{equ} &= \frac{D}{226.2} - 0.1875 \end{aligned}, \tag{3}$$

where P is pressure in MPa, D is the depth below the seafloor in meters, C_{3+4}^{equ} is the feed gas mass fraction of $C_3 + C_4$ that is equilibrium with hydrate at the specified P and the temperature that corresponds to this pressure under Bush Hill.

[17] Negative values of $C_{3+4}^{v\text{-}gas}$ in Figure 3 indicate that the feed gas need contain no hydrocarbons higher than ethane to precipitate Structure II gas hydrate. Gas compositions with negative $C_{3+4}^{v\text{-}gas}$ contents are of course not chemically realistic, but the distance (at constant pressure) between free gas with positive $C_{3+4}^{v\text{-}gas}$ and the solid equilibrium line in Figure 3 is a valid measure of the degree of thermodynamic disequilibrium of that gas with respect to the hydrate it would precipitate at that pressure.

[18] For positive values of $C_{3+4}^{J\text{-}gas}$, Figure 3 predicts the depth below the seafloor at which hydrates will precipitate from gas with the compositions of Jolliet reservoir gas. The range in predicted depths of hydrate precipitation for gas with Jolliet reservoir composition is 573–649 mbsf. These depths are larger than the 260 mbsf and 450 mbsf predicted by vent gas compositions in GC 184/185 by *Milkov and Sassen* [2000]. *Milkov and Sassen* [2000] based their calculations on vent samples V-6 and V-7 in Table 1, chose a bottom water temperature of 8°C, and chose a geothermal gradient of 25°C/km. For these choices we reproduce the hydrate zone thickness they calculate. The thickness of our hydrate zone is greater than their V-7 estimate because we choose a seafloor temperature of 7°C and a geothermal gradient of 20°C/km.

2.3. Relation Between Hydrate and Feed Gas Composition

[19] Prediction of the gas composition of Structure II hydrate is complex. For simple gas hydrate at a given feed gas fugacity, the higher the Langmuir constant the stronger enclathrated the gas component is in the hydrate cavity.

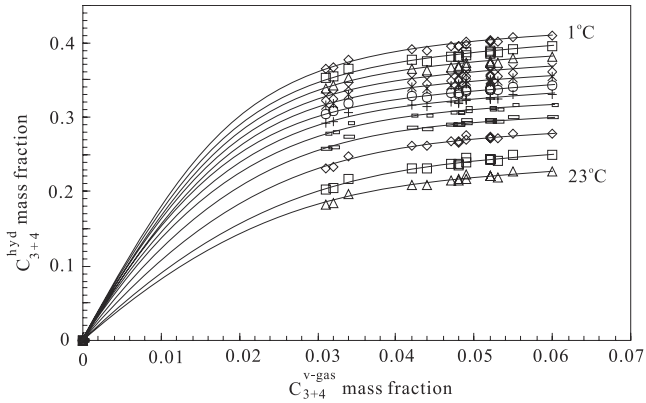

Figure 4. The mass fraction of C_3 plus C_4 in hydrate calculated using the CSMHYD computer program [*Sloan*, 1998] for feed gasses with the composition of the Jolliet reservoir gases at temperatures from 23°C (lowest curve) to 1°C (top curve) (triangle through diamond symbols). The pressures used in the calculations are those encountered below Bush Hill at these temperatures.

Similarly at a given value of the Langmuir constant, higher values of gas fugacity induce a higher fraction of this gas in the hydrate cavity [*Sloan*, 1998]. We again simplify the analysis by considering feed gas with the composition of the measured Jolliet reservoir gases. Figure 4 shows the C_{3+4}^{hyd} compositions of hydrates that would precipitate from venting gas with the composition of the Jolliet reservoir gases at the temperatures and pressures in the subsurface at Bush Hill. The hydrate compositions are calculated using the CSMHYD computer program of *Sloan* [1998] for a pore fluid salinity of 3.45%. We assume that the C_{3+4}^{hyd} of hydrate gas is zero when $C_{3+4}^{v\text{-}gas}$ in Jolliet reservoir gas is zero. With this assumption, C_{3+4}^{hyd} the of gas hydrate and Jolliet reservoir gas are related at an $R^2 > 0.998$:

$$C_{3+4}^{hyd} = b + a_1 C_{3+4}^{v-gas} + a_2 \left(C_{3+4}^{v-gas}\right)^2 + a_3 \left(C_{3+4}^{v-gas}\right)^3, \qquad (4)$$

where, $b = -4. \times 10^{-6} T + 6.0 \times 10^{-5}$, $a_1 = -0.5901T + 24.332$, $a_2 = 14.133T - 491.49$, $a_3 = -108.44T + 3405.9$, T is temperature in °C, and C_{3+4}^{hyd} and $C_{3+4}^{v\text{-}gas}$ are mass fraction of hydrate and vent feed gas respectively.

2.4. A Kinetic Model for Hydrate Precipitation From a Venting Gas Stream

[20] We can now construct a kinetic model for hydrate precipitation beneath Bush Hill. Consider a volume of gas migrating upward toward the seafloor. In a coordinate system moving with the gas, the mass M of a particular packet of gas will decrease with time due to hydrate precipitation:

$$\frac{DM}{Dt} = -k\Delta C \exp\left(\frac{E^*}{R}\left(\frac{1}{T^*} - \frac{1}{T}\right)\right), \qquad (5)$$

where $\Delta C = C_{3+4}^{v\text{-}gas} - C_{3+4}^{equ}$ is the chemical driving force for the hydrate-forming reaction, k is the kinetic rate constant, and the other parameters account for a standard Arhennius rate dependence on temperature. If $\Delta C > 0$, hydrate is precipitated at a rate proportional to k, and the mass of gas is diminished. If $\Delta C < 0$, hydrate (if present) is dissolved, and the mass of the gas packet is increased. In the expression for ΔC, $C_{3+4}^{v\text{-}gas}$ is the $C_3 + C_4$ mass fraction composition of the vent gas, C_{3+4}^{equ} is the $C_3 + C_4$ mass fraction composition of the gas that would be in equilibrium with hydrates precipitating from this gas at the pressure and temperature selected (on solid equilibrium line in Figure 3). In (5)E^* is the activation energy of the reaction, R is the gas constant, T^* is an arbitrary reference temperature which we take to equal 273.15°K, and T is the temperature at the location of the gas packet in °K. The exothermic heat from hydrate precipitation is small and is ignored.

[21] If the gas is migrating vertically with a velocity v_z, we can use the chain rule to convert the time derivative to a spatial derivative. The incremental change in M that will occur as the gas rises a distance Δz is then:

$$\Delta M = -k\Delta C \exp\left(\frac{E^*}{R}\left(\frac{1}{T^*} - \frac{1}{T}\right)\right)\frac{\Delta z}{v_z}, \qquad (6)$$

where $\Delta z/v_z$ is the time to move a vertical distance Δz, and the other variables are defined as in (5) above.

[22] The application of (6) to venting at Bush Hill is illustrated in Figure 5. First equation (3) is used to calculate the depth below the seafloor at which hydrate will begin precipitating for a Jolliet reservoir gas with particular $C_{3+4}^{J\text{-}gas}$ mass fraction. Note that we assume a supply of free gas into the base of hydrate stability, and that hydrate crystallization begins as soon as it is thermodynamically permitted, albeit at possibly a very slow rate. The interval between the depth at which hydrate crystallization begins and the surface is then divided into 10 equal increments. The gas is moved, unchanged in composition (e.g., $C_{3+4}^{v\text{-}gas}(z_1) = C_{3+4}^{J\text{-}gas}$), across the first (deepest) subinterval to z_1[mbsf], and ΔC_1 is calculated for the pressure at this depth (P_1[MPa] = 5.4 + $0.01z_1$[m]) with C_{3+4}^{equ} calculated using equation (3). This value of ΔC_1 is then used in equation (6) to calculate ΔM_1. In this calculation $T_1 = 280.15 + 0.02z_1$, $E^*/R = 10{,}000$ °K, and $K = k\Delta z/v_z$. K is treated as a parametric constant. For a particular choice of K, the original mass of gas is reduced by ΔM_1, and the reduced mass $M_1 - \Delta M_1$ is moved across the next subinterval to z_2 [mbsf].

[23] Conservation of mass requires that the composition of the vent gas at z_2 be changed to reflect the composition of the hydrate precipitated. The mass of C_{3+4} at z_2 minus the mass of C_{3+4} at z_1 must equal the mass of C_{3+4} in the precipitated hydrate. Mathematically:

$$M_1 C_{3-4}^{v-gas}[z_1] - (M_1 - \Delta M_1) C_{3+4}^{v-gas}[z_2] = \Delta M_1 C_{3+4}^{hyd}[z_1].$$

The composition of hydrate precipitated at z_1, $C_{3+4}^{hyd}[z_1]$, is calculated from T_1, P_1, and $C_{3+4}^{v}[z_1]$ using equation (4). The vent gas composition at z_2 is thus determined by rearranging the above equation:

$$C_{3+4}^{v-gas}[z_{i+1}] = \frac{M_i C_{3-4}^{v-gas}[z_i] - \Delta M_i C_{3+4}^{hyd}[z_i]}{M_i - \Delta M_i}, \qquad (7)$$

where we index depth by the subscript i.

[24] This method of calculating the vent gas composition is simply applied to successively higher nodes to obtain a

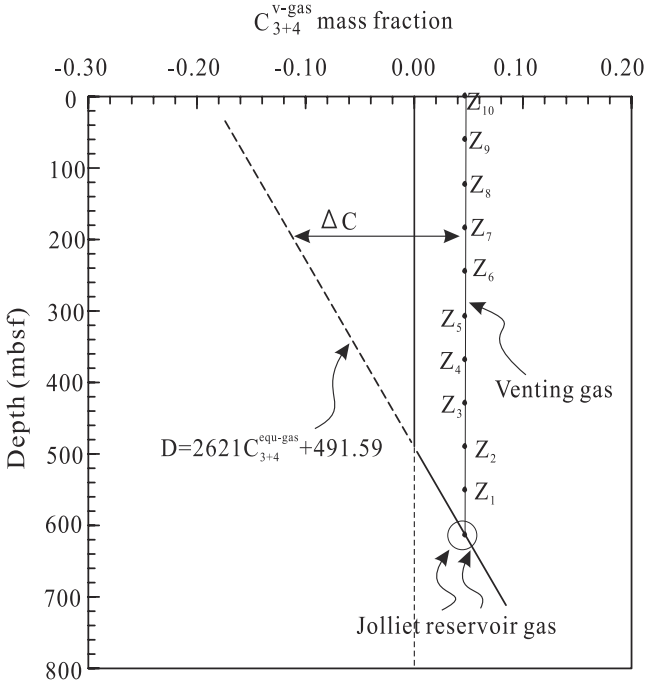

Figure 5. Illustration of method used for calculating the rate of hydrate precipitation beneath Bush Hill. The hydrate phase boundary is represented by the dashed to solid line cutting diagonally across the figure. The light, near-vertical line divided into 10 segments is the hypothetical composition-depth trajectory of a venting Jolliet gas. At any pressure, the distance ΔC between this line and the hydrate phase boundary is a measure of the chemical disequilibrium of the vent gas and the driving force for the hydrate precipitation reaction.

complete solution. The solution at each node is propagated to the next until the surface (tenth subinterval) is reached. For example, knowing $C_{3+4}^{v\text{-}gas}[z_2]$ from the first step, we can calculate $\Delta C[z_2]$ from equation (3), ΔM_2 from equation (6), $C_{3+4}^{hyd}[z_2]$ from equation (4), and $C_{3+4}^{v\text{-}gas}[z_3]$ from equation (7). Then knowing $C_{3+4}^{v\text{-}gas}[z_3]$ we can calculate $\Delta C[z_3]$, ΔM_3, $C_{3+4}^{hyd}[z_3]$, and so on to z_{10}.

2.5. Results for a Base Case Set of Bush Hill Parameters

[25] Figure 6 shows the results of a set of kinetic calculations with the feed gas set equal to the mean of all analyzed Jolliet gases (0.04675) and the kinetic parameter K varying from 0.01 to 0.04 in steps of 0.002. For this feed gas composition, the precipitation of hydrate begins at 614 mbsf. Depending on the value of K, hydrate precipitation causes the $C_3 + C_4$ composition of the gas venting across the seafloor to shift between 0.0425 ($K = 0.002$) and 0.0034 ($K = 0.04$). The range of vent gases K sampled at Bush Hill is 0.013 to 0.049. It is as shown by the range labeled "vent" above the top horizontal axis of Figure 6 (see also Table 1). The range of observed vent gas compositions is almost spanned by the model predictions for venting of an average Jolliet gas if the venting rate is varied by an order of magnitude (such that K changes from 0.002 at high venting rate to 0.02 at low venting rate). The existence of vent analyses with slightly greater $C_3 + C_4$ content than the average Jolliet reservoir gas means that the venting gas might have a $C_3 + C_4$ slightly greater than the average presently analyzed Jolliet gas, that the feed gas composition changed with time, or that propane has biodegraded to some slight degree. The important finding here is that the chemical variation observed in Bush Hill vent gases could be accounted for by an order of magnitude variation in the venting rate of a constant feed gas composition close to the average Jolliet reservoir gas.

[26] Figure 6 also shows the $C_3 + C_4$ mass fraction composition of the hydrate that is precipitated from the model feed gas as it migrates upward to the seafloor from ~614 mbsf. The calculated $C_3 + C_4$ mass fraction of gas hydrate at the seafloor varies from 0.3684 to 0.0146, a range which more than spans the range of hydrate composition observed in Bush Hill samples. The observed range (0.08 to 0.248, Table 1) is shown by the bar labeled "Hydrate" above the top horizontal axis of Figure 6. The range in calculated hydrate composition is much greater than the range in vent composition. Thus, venting a relatively constant composition feed gas at rates varying by about an order of magnitude could explain both the observed range in

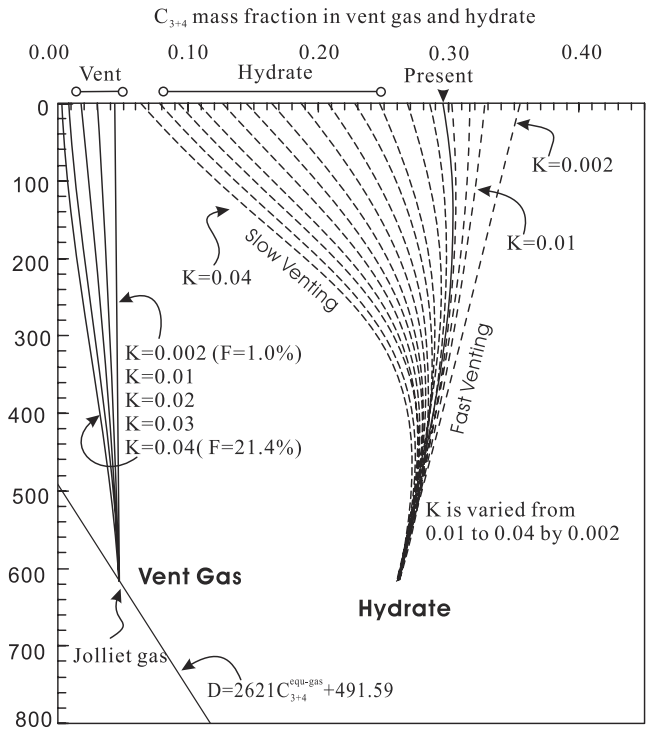

Figure 6. Composition (C_{3+4} mass fraction) of Bush Hill vent gases and hydrates calculated with the kinetic model discussed in text. Calculations are for K values ranging from 0.01 to 0.04 in steps of 0.002. The package of five lines at the left show the C_{3+4} variation of the vent gas as a function of depth. The package of lines on the right show how the C_{3+4} mass fraction of gas in the precipitated hydrate varies with depth. The range of surface Bush Hill vent gases and hydrates are shown at above the top horizontal axis. The hydrate profile corresponding to venting of the mean Jolliet gas at the K value that converts it to the mean observed vent gas is shown by the darker solid line labeled "Present."

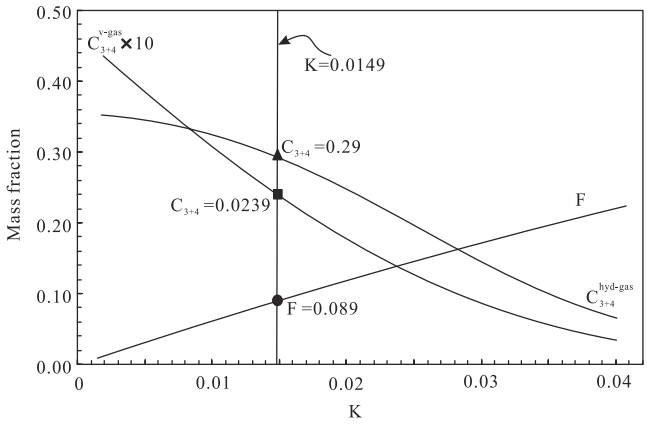

Figure 7. Total mass fraction of venting gas (ΔM) precipitated as hydrate beneath the Bush Hill vents and the C_{3+4} mass fraction compositions of the gases vented and the hydrates precipitated at the seafloor. Vertical line labeled K = 0.0149 shows these parameters for venting the mean C_{3+4} mass fraction of Jolliet reservoir gas (0.04675) at the rate (K = 0.0149) required to produce the mean measured vent gas composition (0.0239). The predicted composition of the hydrates precipitated at the seafloor in this case is 0.029 and ~8.9 wt % of the gas is precipitated as hydrate.

vent gas and the greater observed range in near-surface hydrate compositions. Other factors such as partial biodegradation of the vent gas and bacterial oxidation of gas hydrate could also explain some of the hydrate composition variation.

[27] The mass fraction ($F = \Delta M/M_o$) of venting gas enclathrated in gas hydrate in the calculations shown in Figure 7 varies from 0.013 (at K = 0.002) to 0.22 (at K = 0.04). The model vents gas with the mean Bush Hill vent gas composition (0.0239) when K = 0.015. At K = 0.015 the mass fraction of venting gas precipitated as hydrate at is 0.089. Typically, therefore, the Bush Hill system precipitates about 9 wt % of its feed gas as hydrate below the surface, and about 91 wt % of the feed gas is vented. These figures are confirmed in another way in Tables 2 and 3. Table 2 shows the K values required to convert each measured Jolliet reservoir gas to an observed Bush Hill vent gas. Where the vent gas has composition richer in than the reservoir gas, the K value is assigned an "N". The conversion K values range from 0 to 0.0311, but the mean value of the mean conversion K (lower left entry in Table 2) is 0.0160. Table 3 shows the mass fraction precipitated as hydrate corresponding to the Table 2 numbers. The range in the gas mass fractions precipitated as hydrate is 0 to 19 wt %, but the mean of the mean estimates (lower left table entry) is 9.5 wt %. We again conclude that typically about 9% of the gas precipitates as hydrate in the Bush Hill subsurface.

[28] Figure 6 makes an important prediction that could allow testing of our kinetic model. It suggests that, provided the feed gas composition is relatively constant, the range in the $C_3 + C_4$ hydrate composition may narrow dramatically with depth and it predicts that this narrowing should occur through an increase in the $C_3 + C_4$ content of the lower bound of the range in hydrate composition. Variability in feed gas composition would cause the composition of the hydrates near the base of the hydrate layer to vary correspondingly. Drilling the Bush Hill vent to ~620 mbsf could test the predicted depth-dependence of hydrate composition and also determine the variability of feed gas composition. The range of hydrate composition should narrow to the range of feed gas variability as the base of hydrate crystallization is approached.

[29] Figure 7 summarizes the relationships between K, the mass fraction of hydrate precipitated from the venting gas, the composition of gas venting into the ocean, and the composition of hydrate precipitating near the seafloor. This figure shows that the surface hydrate mass fraction $C_3 + C_4$ is ~0.31 at the K value (0.015) that fits the mean present $C_3 + C_4$ vent gas composition of 0.0239. This hydrate

Table 2. Tabulation of Kinetic K Values Required to Convert the C_{3+4} Mass Fraction in Jolliet Gases to the C_{3+4} Mass Fraction of Vent Gases at Bush Hill in GC 185[a]

Jolliet	Vent Content	V-1 0.024	V-2 0.02	V-3 0.013	V-4 0.013	V-5 0.034	V-6 0.049	V-7 0.015	V-8 0.023	Mean 0.0239
J-1	0.032	0.0059	0.0091	0.0160	0.0160	N	N	0.0138	0.0066	0.0084
J-2	0.031	0.0052	0.0085	0.0154	0.0154	N	N	0.0132	0.0060	0.0079
J-3	0.052	0.0177	0.0208	0.0272	0.0272	0.0109	0.0017	0.0252	0.0184	0.0186
J-4	0.049	0.0161	0.0192	0.0256	0.0256	0.0092	N	0.0236	0.0168	0.0170
J-5	0.047	0.0150	0.0181	0.0246	0.0246	0.0080	N	0.0225	0.0157	0.0161
J-6	0.048	0.0155	0.0186	0.0251	0.0251	0.0086	N	0.0231	0.0163	0.0165
J-7	0.052	0.0177	0.0208	0.0272	0.0272	0.0109	0.0017	0.0252	0.0184	0.0186
J-8	0.034	0.0072	0.0104	0.0172	0.0172	N	N	0.0151	0.0080	0.0094
J-9	0.048	0.0155	0.0186	0.0251	0.0251	0.0086	N	0.0231	0.0163	0.0165
J-10	0.044	0.0132	0.0164	0.0230	0.0230	0.0063	N	0.0209	0.0140	0.0146
J-11	0.06	0.0219	0.0249	0.0311	0.0311	0.0152	0.0062	0.0292	0.0226	0.0228
J-12	0.042	0.0121	0.0153	0.0219	0.0219	0.0051	N	0.0198	0.0129	0.0136
J-13	0.053	0.0182	0.0213	0.0277	0.0277	0.0114	0.0023	0.0257	0.0190	0.0192
J-14	0.055	0.0193	0.0224	0.0287	0.0287	0.0125	0.0035	0.0267	0.0200	0.0202
J-15	0.049	0.0161	0.0192	0.0256	0.0256	0.0092	N	0.0236	0.0168	0.0170
J-16	0.052	0.0177	0.0208	0.0272	0.0272	0.0109	0.0017	0.0252	0.0184	0.0186
Mean	0.04675	0.0146	0.0178	0.0243	0.0243	0.0079	0.0011	0.0222	0.0154	0.0160

[a] K values are defined in discussion following equation (6) in the text. Jolliet gases, J-1 through J-16 with values in second column; Bush Hill vent gases in GC 185, V-1 through V-8 with values in second row. An entry "N" is entered where the vent gas is richer in C_{3+4} than the corresponding Jolliet reservoir gas and hydrate precipitation cannot achieve the conversion.

Table 3. Mass Fraction of Venting Jolliet Reservoir Gas That Must be Precipitated as Hydrates to Produce Bush Hill Vent Gas[a]

Jolliet	Vent Content	V-1 0.024	V-2 0.02	V-3 0.013	V-4 0.013	V-5 0.034	V-6 0.049	V-7 0.015	V-8 0.023	Mean 0.0239
J-1	0.032	0.0331	0.0503	0.0860	0.0860	N	N	0.0750	0.0369	0.0459
J-2	0.031	0.0287	0.0465	0.0822	0.0822	N	N	0.0711	0.0330	0.0430
J-3	0.052	0.1087	0.1260	0.1606	0.1606	0.0687	0.0115	0.1499	0.1129	0.1124
J-4	0.049	0.0972	0.1146	0.1493	0.1493	0.0572	N	0.1386	0.1014	0.1009
J-5	0.047	0.0896	0.1070	0.1418	0.1418	0.0496	N	0.1311	0.0938	0.0943
J-6	0.048	0.0934	0.1108	0.1456	0.1456	0.0534	N	0.1348	0.0976	0.0976
J-7	0.052	0.1087	0.1260	0.1606	0.1606	0.0687	0.0115	0.1499	0.1129	0.1124
J-8	0.034	0.0404	0.0580	0.0936	0.0936	N	N	0.0826	0.0447	0.0516
J-9	0.048	0.0934	0.1108	0.1456	0.1456	0.0534	N	0.1348	0.0976	0.0976
J-10	0.044	0.0783	0.0957	0.1307	0.1307	0.0382	N	0.1199	0.0825	0.0845
J-11	0.06	0.1397	0.1569	0.1912	0.1912	0.0998	0.0424	0.1807	0.1439	0.1432
J-12	0.042	0.0707	0.0882	0.1233	0.1233	0.0306	N	0.1124	0.0750	0.0779
J-13	0.053	0.1125	0.1298	0.1644	0.1644	0.0726	0.0153	0.1537	0.1167	0.1162
J-14	0.055	0.1202	0.1375	0.1720	0.1720	0.0803	0.0230	0.1614	0.1244	0.1239
J-15	0.049	0.0972	0.1146	0.1493	0.1493	0.0572	N	0.1386	0.1014	0.1009
J-16	0.052	0.1087	0.1260	0.1606	0.1606	0.0687	0.0115	0.1499	0.1129	0.1124
Mean	0.04675	0.0888	0.1062	0.1410	0.1410	0.0499	0.0072	0.1303	0.0930	0.0947

[a]Jolliet reservoir gas, J-1 through J-16; Bush Hill vent gas, V-1 through V-8. Mass fractions correspond to the K values in Table 2. "N" indicates vent gas is richer in C_{3+4} than the corresponding Jolliet reservoir gas and hydrate precipitation cannot convert the reservoir gas to vent gas.

composition is above the upper end of range of the observed surface hydrate $C_3 + C_4$ mass fractions at Bush Hill, as indicated by the position of "present" hydrate precipitation curve relative to the observed "Hydrate" bar above the top horizontal axis in Figure 6. Most of the hydrate samples that have been collected from Bush Hill have $C_3 + C_4$ mass fractions lower than we would predict from the venting rates (0.002 to 0.02) that match most of the vent gas compositions measured at Bush Hill. The vent gases reflect conditions in the last decade when the samples were collected, while the hydrate samples could reflect conditions in the considerably more distant past. This may suggest that the present (last decade) venting rates have been greater in the past.

[30] Figure 7 shows that the fraction of gas precipitated as hydrate is directly proportional to K, and therefore inversely proportional to venting rate. This means that, according to our model, the hydrate accumulation rate at Bush Hill is largely independent of the venting rate over a considerable range of gas discharge rates. The Bush Hill hydrates should have accumulated at a steady rate despite any changes in venting rate that may have occurred there.

[31] Figure 8 shows how vent gas mass is lost to hydrate as a function of depth and how hydrate volume will accumulate at constant hydrate density. Except near the base of the hydrate precipitation zone, below 500 m, the mass of vent gas crystallized to hydrate per meter depth is approximately constant for venting rates near the current average (K = 0.015). Hydrate mass and volume should accumulate fairly evenly with depth to about 500 mbsf, and then taper to zero at 614 m.

[32] Using the hydrate crystallization profile for K = 0.015 in Figure 8, we can project the near-surface hydrate volumes observed at Bush Hill to depth, and integrate to obtain an estimate of the total hydrate volume. Figure 9 shows a seismic image of the upper few 10 s of meters of the Bush Hill hydrate mound. The mound is about 800 m in diameter at its base and rises 19 m above the seafloor. If we assume the mound is 2 vol % hydrate, which is the hydrate content of Blake Ridge sediments estimated by geochemical and geophysical methods [*Egeberg and Dickens*, 1999; *Helgerud et al.*, 2000; *Collect and Lee*, 2000], the model volume-depth profile for K = 0.015 in Figure 8 suggests the total hydrate volume at the Bush Hill vent is $\sim 6.2 \times 10^6$ m^3. For ratio of gas volume at STP to Structure II hydrate volume of 180 [*Sloan*, 1998], the corresponding volume of gas tied up in hydrate is $\sim 1.1 \times 10^9$ m^3. This is similar to the volume of gas in the Jolliet reservoirs. The Jolliet reservoirs contain 4.3×10^9 m^3 (152 bcf) of gas.

[33] The time interval over which the Bush Hill hydrates accumulated can be estimated in several ways. *Roberts and Aharon* [1994] radiometrically dated samples of Bush Hill carbonates and found ages ranging from 1.4 to 3.2 ka. The Jolliet Reservoir gases are sealed and compartmented by normal faults, which attained their present configuration in late Pleistocene to Holocene time [*Cook and D'Onfro*, 1991]. Recent migration and accumulation is also suggested by the lower-than-expected levels of biodegradation of the gases in the shallow, cool Jolliet Reservoirs. If the Bush Hill hydrates accumulated over the last 10,000 years by removing ~9% of a vent gas stream, the average gas venting rate at Bush Hill would have been $\sim 1.3 \times 10^6$ m^3/yr (0.9×10^6 kg/yr) over the last 10,000 years. This venting rate is similar to the filling rate of the Jolliet reservoirs. If the reservoirs filled in the last 10,000 years, their average filling rate would have been 0.43×10^6 m^3/yr.

[34] Gas venting at Bush Hill has been measured by capturing bubble streams at individual sites on the mound. The local bubbling rate is typically 30 to 60 cm^3/minute or ~20 m^3/year [*Roberts*, 2001; *Sassen et al.*, 2001b]. This is a compressed gas volume rate. Decompressing ~20 m^3/year from 540 bars to 1 bar gives a venting rate of $\sim 10^4$ m^3/yr. *Sassen et al.* [2001b] estimate venting from a single site on the Bush Hill mound at 3×10^4 m^3/yr STP. The base of the dramatic gas plume recorded by Roberts August 2000 visit to the site [*Roberts*, 2001; *Sassen et al.*, 2001a] is ~600 m wide and centered on the 800 m diameter Bush Hill hydrate mound. Approximately 100 such bubble streams venting 10^4 m^3/yr over the 600 m diameter active zone of Bush Hill mound (e.g., bubble streams spaced about 60 m apart) would be required to produce a total discharge of 10^6 m^3/year. Submersible observations suggest the venting rate

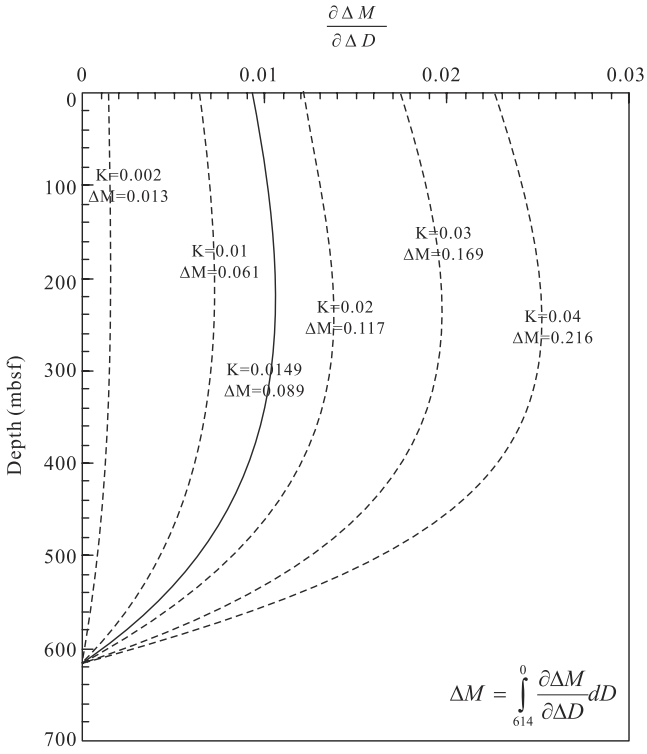

Figure 8. Predicted mass fraction of vented gas precipitated per meter depth plotted as a function of depth for selected kinetic (K) values. Venting of the mean Jolliet reservoir gas at the rate required to produce the mean vent gas C_{3+4} composition is the solid curve. For constant venting conditions (constant K values) each profile indicates how the hydrate mass will be distributed with depth. The figure suggests hydrates will be distributed evenly with depth to near the base of the hydrate layer.

is highly variable on the mound. There may be diffuse as well as focused leakage. All considered a cumulative venting rate of 10^6 m^3/year over the entire mound is reasonable (H. Roberts, personal communication, 2001). If our calculated $\sim 1.2 \times 10^6$ m^3/year venting is spread uniformly across a 600 m diameter circular footprint, the venting rate per unit area is $\sim$4.6 m^3 STP gas/m^2-year.

2.6. Parametric Variations From the Base Case Bush Hill Parameter Values

[35] While we have selected the most likely parameter values for Bush Hill, there is or course some uncertainty in the values selected. The bottom water temperature may not have been 7°C on average, for example, and the literature contains the (we believe erroneous) notion that the subsurface temperature gradient at Bush Hill is 25°C/km rather than 20°C/km. Other sites would have different bottom water temperatures and subsurface temperature gradients. The Bush Hill hydrate mound could easily contain 5 vol % rather than 2 vol % hydrate. For many reasons it is of interest to determine the impact of reasonable parameter changes on gas venting rates, hydrate accumulation rates, and mound hydrate content. Table 4 and Figures 10 and 11 report the results of a series of calculations in which the bottom water temperature is varied from 5° to 13°C, the subsurface temperature gradient from 15° to 50°C/km, and the hydrate content of the Bush Hill mound (and its subsurface extension) is either 2 or 5% by volume.

[36] Table 4 shows that as the average surface temperature increases from 5° to 13°C, the fraction subsurface gas precipitation that is required to convert Jolliet reservoir gas to the sampled vent composition increases $\sim$5% (from 0.88 to 0.92), the venting rate required to effect this precipitation drops by a factor of 4.3 (from 1.4 to 0.3 $\times$ 10^6 m^3/yr), and the hydrate volume in the subsurface drops by the same factor (from 7.5 to 1.8 $\times$ 10^9 m^3). This all makes good sense. The fractional precipitation, F, changes little because the partitioning between gas and hydrate is not very sensitive to small temperature changes. The venting rate must be slowed dramatically, however, because crystallization must occur over a smaller depth range. Since the depth at which hydrate is stable depends on pressure as well as temperature, the effects of surface temperature increases are compounded. Precipitating the same fraction of gas in the same time period but over a shorter depth interval (column 2 of Table 4) necessarily accumulates less hydrate.

[37] Table 4 shows that as the subsurface temperature gradient increases from 15° to 50°C/km (at a constant seafloor temperature of 7°C), the fraction of gas, F, precipitated as hydrate remains virtually unchanged while the venting rate and hydrate accumulation over 10,000 years decrease by a factor of $\sim$4.2. Again, this is reasonable. Since the chemical partitioning between gas and hydrate is much less sensitive to pressure than temperature, changing the subsurface temperature gradient mainly means that the venting gas stream has a different depth interval over which to precipitate hydrate. The kinetics are unchanged if the transit time across the hydrate zone is the same. Hence

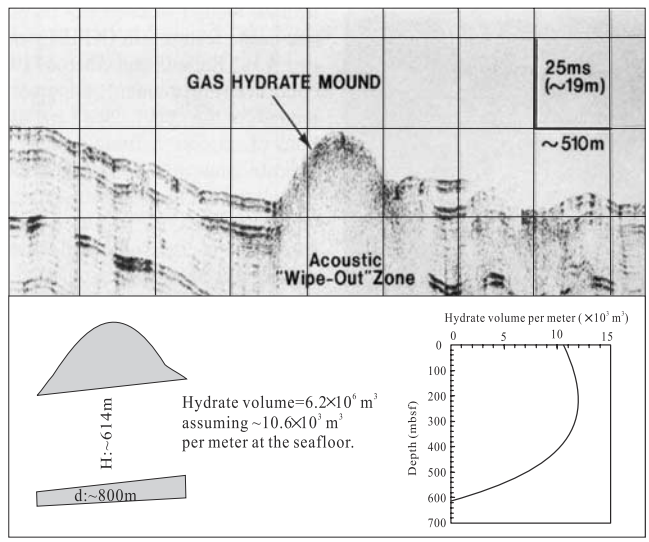

Figure 9. High-resolution seismic profile across the gas hydrate mound in GC 185. The inserts indicate how the profiles in Figure 8 can be used to extrapolate the hydrate surface mass to depth to estimate a total hydrate volume at Bush Hill of 6.2 $\times$ 10^6 m^3. A constant hydrate density of $\sim$0.93 [*Sloan*, 1998] is used in this calculation. The seismic profile in the upper part of the figure is modified from *Roberts and Carney* [1997].

Table 4. Summary of Parameters for Which the Jolliet Reservoir Gas Mass Fraction $C_3 + C_4 = 0.0465$ is Vented at the Composition of the Average Sampled Bush Hill ($C_3 + C_4 = 0.0239$) Vent Gas[a]

Variable Seafloor T at $\partial T/\partial z$ = 20°C/km	D, mbsf	K	F	Venting Rate, 10^6 m^3/yr		Hydrate Volume, 10^6 m^3	
				2 Vol %	5 Vol %	2 Vol %	5 Vol %
5	741	0.0114	0.088	1.4	3. 5	7.5	18.8
7	614	0.0149	0.089	1.2	2.9	6.2	15.6
7 (20 nodes)	614	0.0481	0.086	1.2	3.0	6.2	15.6
7 (“& E^*/R = 2500)	614	0.0082	0.088	1.2	2.9	6.2	15.6
9	478	0.0211	0.090	0.9	2.2	4.9	12.2
11	332	0.0348	0.092	0.6	1.5	3.4	8.5
13	175	0.0900	0.092	0.3	0.8	1.8	4.6
Variable $\partial T/\partial z$ at seafloor T = 7°C							
15	893	0.0125	0.086	1.7	4.3	9.0	22.6
20	614	0.0149	0.089	1.2	2.9	6.2	15.6
25	464	0.0160	0.088	0.9	2. 2	4.7	11.8
30	372	0.0167	0.087	0.7	1.7	3.8	9.5
35	310	0.0173	0.087	0.6	1. 5	3.2	8.0
40	266	0.0178	0.087	0.5	1. 3	2.7	6.9
45	232	0.0181	0.086	0.5	1.1	2.4	6.0
50	206	0.0183	0.086	0.4	1.0	2.1	5.3

[a] D = maximum depth of hydrate crystallization; K = computational kinetic rate constant; $F = \Delta M/M_o$ = the mass fraction of venting gas precipitated as hydrate. Venting rate and subsurface hydrate volume are shown for 2 and 5 vol % hydrate in the Bush Hill hydrate mound and its subsurface extensions. Three calculations are reported for 7° and 20°C/km: 10 nodes and E^*/R = 10,000°C, 20 nodes and E^*/R = 10,000°C, and 20 nodes and E^*/R = 2500°C.

venting rate and hydrate accumulation vary inversely with the hydrate layer thickness (column 2 in Table 4).

[38] Finally the venting rate and volume of gas accumulated as hydrate in the subsurface are both very sensitive to the volume percent hydrate in the Bush Hill mound (and its subsurface extension). The volume of subsurface hydrate must increase as the hydrate content of the sediments increases. At the same fraction gas crystallization and the same time interval, the gas venting rate must increase to supply the increased subsurface hydrate volume.

[39] Figures 9 and 10 plot the data in Table 4. The fraction of gas precipitated as hydrate changes little for reasonable changes in seafloor temperature and subsurface temperature gradient. Venting rate and the volume of gas accumulated as subsurface hydrate vary directly with the inverse of the subsurface temperature gradient, and inversely with seafloor temperature.

3. Discussion of the Kinetic Model

[40] The kinetic model we construct differs dramatically from the current hydrate models in the literature. The model published recently by *Xu and Ruppel* [1999] is the latest version of the current modeling approach. It investigates hydrate accumulation using conservation equations of heat, momentum, and methane mass balance. Their model assumes dissolved methane in the methane hydrate zone is in equilibrium with hydrate. Following *Rempel and Buffett* [1997], the kinetics of hydrate precipitation are assumed to be fast enough that kinetic constraints on hydrate accumulation can be ignored, and by default the rate of accumulation is controlled by mass and heat transport. There is no free gas in the hydrate stability zone. Their models are appropriate for locations of diffuse methane leakage and particularly for the Blake Ridge, and their main focus is on simulating the top and bottom of the zone where methane hydrate is present, and the depth of the free gas zone, which they show can lie below or at the base of the methane hydrate zone. Uncertainties of a few degrees in the boundary of the hydrate stability zone can be important [*Ruppel*, 1997]. In contrast, the rate of hydrate precipitation in our model is kinetically controlled, we have a free gas phase throughout the hydrate stability zone, there is no top to our hydrate zone (methane gas vents the surface, and hydrate precipitates at the surface), our mass transport is simplified to a single phase gas stream from which hydrate precipitates, and uncertainties of a few degrees in the hydrate stability zone are not important. Our model is appropriate for areas where gas is venting (such as Bush Hill), and in a sense represents a complimentary end-member model to that constructed by *Xu and Ruppel* [1999].

[41] The kinetic model represented by equation (6) is simplified in several ways. (1) It assumes hydrate precipitation can be characterized by a first order, linear kinetic

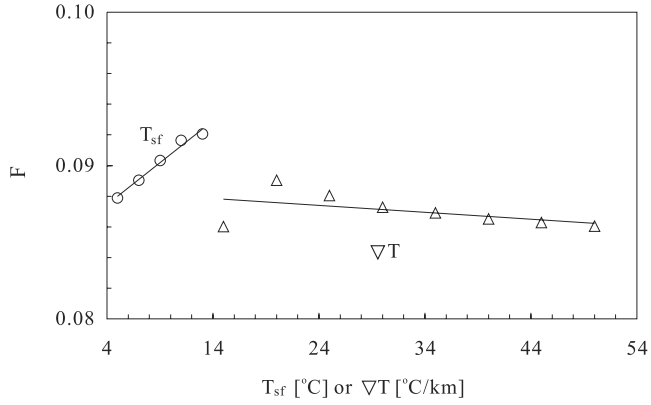

Figure 10. The mass fraction of venting gas precipitated as hydrate, F, that is required to convert the average Jolliet reservoir gas composition to that of the average Bush Hill vent gas is plotted: (1) for a subsurface temperature gradient ∇T = 20°C/km as a function the average seafloor temperature, T_{SF}, and (2) for a surface temperature of 7°C as a function of ∇T. Data are from Table 4.

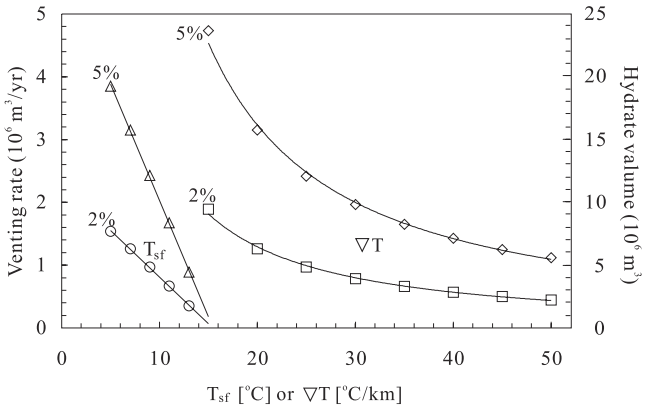

Figure 11. Calculated venting rates and subsurface gas volumes stored as hydrate are plotted against seafloor temperature (for ∇T = 20°C/km) and ∇T (for T_{SF} = 7°C). The calculations are constrained such that the average Jolliet reservoir gas vents at the average Bush Hill vent gas composition. Curves are shown assuming the Bush Hill hydrate mound contains 2 and 5 vol % hydrate. Data are from Table 4.

model. (2) It assumes that the degree of chemical disequilibrium (the chemical driving force for the reaction) can be represented by the difference between the mass fraction of $C_3 + C_4$ in the free gas phase and the (possibly negative) free gas composition that would be in equilibrium with hydrates precipitating at the defined pressure and temperature. (3) It assumes that the activation energy is similar to that characterizing solid phase reactions in which E^*/R = ~10,000°K and therefore that the hydrate precipitation reaction is controlled by solid surface processes and not the diffusion of methane away from gas bubbles, a process that would have an activation energy characterized by E^*/R values closer to 2,500°K. In the current literature vernacular we assume porous media kinetics rather than open system kinetics. (4) The kinetic constant K ($=k\ \Delta z/v_z$) is assumed not to vary with depth. Thus both the gas venting velocity and the kinetic rate constant k are assumed not to change with depth. (5) The subsurface temperature profile is assumed to be constant. Flow does not perturb the temperature gradient in our models, and the surface temperature in our simulations is constant. (6) Because the temperature profile is constant, we model only hydrate precipitation.

[42] Several of these simplifications can be quantitatively justified. If E^*/R is ~2500°K rather than ~10,000°K, the value of K required to convert the mean Jolliet gas to the mean venting gas composition is changed by a factor of ~3, but, as shown in Table 4, the percent gas precipitated as hydrate, the volume of hydrate accumulated in the subsurface, and the venting rates are changed very little. Since this change in the activation energy is about as extreme as can be imagined, plausible precipitation mechanisms (e.g., open system/direct-crystallization from a gas bubbles versus porous media/crystallization onto a solid surface) give the same results in our empirically calibrated kinetic model.

[43] We know that rapid pulses in venting associated with mud volcanoes can increase the surface temperature of the muds at the surface by up to 10°C [*Roberts*, 2001]. Bottom water temperature variations could also decompose hydrates. *Sassen et al.* [2001a] state, however, that the vent gas at Bush Hill shows no significant evidence of hydrate decomposition. Hydrate decomposition could matter elsewhere but it does seem to be a concern at Bush Hill.

[44] The remaining assumptions address the foundations of the kinetic model itself. We characterize the chemical driving force for hydrate precipitation by the mass fraction of $C_3 + C_4$ in the free gas phase. Even accepting this is fully appropriate, important details are complex and uncertain. For example, gas velocity is unlikely to be constant with depth. It will be rapid at constrictions and slower where flow spreads out. Hydrate surface area will not be constant with depth. A first order crystallization rate constant is proportional to the hydrate surface area. Capillary forces could be important in nucleating and promoting hydrate precipitation [*Melnikov and Nesterov*, 1996; *Clennell et al.*, 1999, 2000]. We ignore the initial nucleation of hydrate and all effects of interfacial tension in our model. In short our model is highly simplified. Many of the complexities could average out over time as the flow channels shift position. But the main justification is that an unsimplified model would require too much detailed subsurface data to implement. We construct a simple model and empirically calibrate it to the Bush Hill Site. The main assumption we make is that the model can predict the composition of hydrates precipitated in the deeper parts of the vent system.

[45] We have examined model convergence by calculating models with twice the number of nodes so that the interval between nodes in reduced in half (see Figure 5). Table 4 shows that for 20 nodes the mass fraction that must be crystallized from mean Jolliet gas to produce the mean vent gas composition is reduced by ~1% from the 10-node calculation shown in Figure 6. This difference is not significant. The number of nodes used in our calculations is computationally adequate.

[46] Our kinetic model is calibrated to Bush Hill. It cannot be assumed that the regressions equations (1) and (4) are valid everywhere, although they are probably valid for sites near Bush Hill that are in the same hydrocarbon system.

4. Implications of the Application to Bush Hill

[47] The style of thermogenic hydrate accumulation in the Gulf of Mexico is very different from the style of hydrate accumulation on most ocean slopes. In most places, hydrates are associated with bottom-simulating seismic reflectors (BSRs) and faults are not of controlling importance. In the Gulf hydrates BSRs are not observed, and hydrate accumulations are almost invariably associated with faults.

[48] The fault-related thermogenic gas hydrates of the Gulf of Mexico are crystallized from a mass flux of methane that is ~10^3 times greater than that associated with BSR hydrates. BSRs are thought to be caused by gas accumulations below the zone where hydrates have crystallized. Observations and models such as those developed by *Xu and Ruppel* [1999] show that aqueous gas diffusion frequently causes the top of gas to lie below the bottom of the zone of hydrate crystallization. The separation provides a measure of the rate of methane venting. At 1 km water

Table 5. Summary of Bush Hill Parameters Derived or Discussed in the Text

	Vol % Hydrate in Bush Hill Mound		
	2	5	
Hydrate volume, 10^6 m^3	6.2	15.6	
STP Gas volume in hydrate, 10^9 m^3	1.1	2.8	4.3 in Jolliet Reservoirs
STP Gas volume vented in last 10^4 years, 10^9 m^3	11.7	29.8	
Venting rate Bush Hill, 10^6 m^3/yr	1.2	3.0	0.03 single bubble stream
Venting rate Bush Hill, 10^6 kg/yr	0.9	2.1	
Mass Flux 600 m diam. BH Site, kg/m^2 yr	3.2	7.4	$\sim 3 \times 10^{-3}$ in BSR sites

depth and fluid fluxes of 2 mm/yr (which is ~2 times greater than could be produced by compaction in Bush Hill area where sediments are accumulating at <2 mm/yr), Xu and Ruppel's model shows that a methane flux rate of 1.9×10^{-4} kg/m^2 is required to crystallize hydrate, and a methane flux of 3×10^{-3} kg/m^2 yr is required for the top of gas to become coincident with the bottom of hydrate crystallization. Since the top of gas is thought to lie below the bottom of hydrate in many areas, this latter flux provides a rough upper bound estimate on the common rate of gas venting in BSR systems. It is interesting in this context that the gas flux rates we estimate at Bush Hill are more than 10^3 times larger. The STP density of methane is 0.71 kg/m^3. The mass venting rate corresponding to methane fluxes of 4.6–11.3 m^3/year (the base case estimates for 2 and 5 vol % hydrate in the Bush Hill mound) and is therefore 3.2–7.4 kg/m^2 yr, which exceeds the methane flux in BSR systems (3×10^{-3} kg/m^2 yr) by more than three orders of magnitude.

[49] Our model suggests that the methane venting rates at Bush Hill have varied by at least a factor of 3 over the ~10 years that gas samples have been collected there. The venting rate changes significantly on a scale of years. This is shown by the variation in K that is required to span the observation bar labeled "vent" at the top of Figure 6. The variations in hydrate composition (Figure 6) suggest that these changes have been going on for thousands of years, since the hydrates may be at least this old. The compositional changes could also be caused if different parts of the compositionally heterogeneous Jolliet reservoirs vented at the same rate but at different times over the span of a few years. Direct confirmation of variable venting rates by seafloor vent monitoring or repeat echo sounder plume surveying could provide data to test our hypothesis that variable venting rate is the main cause of the variations in gas chemistry.

[50] The volume of gas that our model suggests may be stored in the vent system is surprisingly large. If the hydrate in the Bush Hill mound contains 5 vol % hydrate, the model subsurface fault plumbing system contains $\sim 15.6 \times 10^6$ m^3 hydrate or $\sim 2.8 \times 10^9$ m^3 gas at STP (see Table 5). This is more than half the 4.3×10^9 m^3 of gas contained in the Jolliet reservoirs. Despite uncertainties, the volume hydrate estimate may be quite robust. A certain amount of hydrate crystallization is required to shift the source gas composition to that of the vent gases. If this is done preferentially in the shallow, low temperature subsurface, the amount of crystallization may be reduced, but if the crystallization profile is at all similar to that shown in Figure 8, the change should be small.

[51] The Bush Hill example suggests it may be possible to estimate the subsurface hydrate volume from surface observations in cases where the feed gas composition is not known. As shown in Figure 6, the vent gas samples with the most $C_3 + C_4$ quite faithfully reflect the feed gas composition. The fraction gas precipitated in the subsurface might thus be determined by a model in which the feed gas is taken to be the heaviest sampled vent gas. The fractional precipitation would be that which is required to convert this feed gas to the average vent gas composition. The size of the subsurface hydrate resource could then be estimated from the average seafloor temperature, the subsurface thermal gradient, and geological or geochemical estimates of the duration of venting. Such "no drilling" estimates of hydrate volume could be useful in assessing the economics of hydrate recovery.

[52] While the model may define the hydrate volume as a function of depth in a fault plumbing system, it does not specify the lateral distribution of hydrate in the fault, which could be complex. Determining of how the envelope of hydrate composition changes with depth and whether it is similar to that shown in Figure 6 could provide added confidence in the model and the volume estimates.

[53] Since the venting rate and subsurface hydrate volume are directly related (see Table 4 and Figure 11), defining subsurface hydrate volume directly translates to defining the cumulative amount of methane vented, which is of potential environmental interest. If our model is valid, this is a case where subsurface resources and the venting of greenhouse gases are equivalent measures of the same process. The volume of vented gas equals the subsurface volume of gas stored in hydrate times $(1-F)/F$, where F is the time average mass fraction of gas precipitated as hydrate.

5. Summary and Conclusions

[54] This paper constructs a kinetic model for hydrate precipitation beneath the Bush Hill hydrate mound, Green Canyon 185, offshore Louisiana. The model is based on the composition of the Jolliet reservoir gases. These gases, or gases from the same source, provide the feed gas for the hydrate precipitation and venting at Bush Hill. Chemical disequilibrium in the kinetic model is measured by the difference between the mass fraction of $C_3 + C_4$ in the vent gas and their mass fraction in gas that is in equilibrium with hydrates at the same location (Figure 3). The composition of precipitating hydrate is determined by regressing thermodynamic predictions for the Jolliet reservoir gases (Figure 4). All thermodynamic calculations are carried out using the CSMHYD computer program of *Sloan* [1998].

[55] Vent gas composition, hydrate composition, and the fraction of gas precipitated as hydrate are computed in the Bush Hill vent system using a propagator solution technique (Figure 5). The calculations show (Figures 6 and 7) that the

range in both vent gas and hydrate composition can be accounted for if the feed gas is slightly richer in mass fraction of $C_3 + C_4$ than the mean Jolliet gas, and the venting rate varies by more than a factor of 3 over short ($\sim$1 year) time intervals. The weight percent gas precipitated as hydrate is inversely proportional to venting rate and has varied at Bush Hill from almost zero to $\sim$19%. The average is $\sim$9%. For the average venting rate indicated by the vent gas and hydrate chemistries, about equal amounts of gas are precipitated as hydrate in each depth interval until the base of the hydrate layer is approached (Figure 8).

[56] Using the present-day profile in Figure 8, and assuming the Bush Hill mound contains between 2 and 5 volume percent hydrate, we estimate the total volume of hydrate in and below Bush Hill is $\sim$ 6.2 to 15.6 $\times$ 10^6 m^3 (Table 5). If this hydrate represents 9% of the venting gas, and accumulated over a 10,000 period, the gas venting rate has been between 1.2 and 3.0 $\times$ 10^6 m^3/yr. Up to half as much gas as has been stored the Jolliet reservoirs has crystallized as hydrate between 614 mbsf, and $\sim$5 times more gas has been vented. If the venting is fairly uniform over the 600 m diameter Bush Hill mound, the average gas mass flux has been between 3.2 and 7.4 kg/m^2 yr. This is consistent with seafloor gas venting observations. It $>10^3$ times the estimates of methane fluxes in hydrate accumulations associated with bottom-simulating reflectors where faults are not a factor.

[57] The total volume of gas vented is reflected in the amount stored as hydrate in the subsurface. Measuring one measures the other if the mass fraction of gas that precipitates as hydrate can be inferred. If Bush Hill is a valid guide, it may be possible to estimate subsurface hydrate accumulations (and the cumulative gas vented) from the difference between the $C_3 + C_4$ content of the richest and average gas samples, the local bottom water temperature, the subsurface thermal gradient, an estimate of the duration of venting, and an estimate of the hydrate volume of hydrate with a few meters of the surface (Figures 6 and 9–11).

[58] Our model could be supported by verifying that venting rates vary by a factor of $\sim$3 over a few years at Bush Hill, and by verifying that the range of hydrate $C_3 + C_4$ gas composition changes with depth as shown in Figure 6. The parameter with the most impact on our results is the volume percent hydrate in the Bush Hill mound.

[59] **Acknowledgments.** D. F. Chen acknowledges the support of the NSFC (project 40072044) and the Chinese Academy of Sciences (project KZCX2-SW-117). Funds from the corporate sponsors of the Global Basins Research Network supported D. F. Chen in the U.S. L. M. Cathles is grateful to H. Roberts and the Minerals Management Service for encouragement of the work, especially for an invitation to participate in the submersible investigation of Bush Hill and other areas. The echo sounding images of the venting at Bush Hill mentioned in the text were obtained on this cruise. Steven Losh provided geologic background data and helped compile the geochemical data. Roger Sassen and Carolyn Ruppel provided very helpful and detailed reviews that stimulated significant improvements in the manuscript. We also thank AGU Associate Editor Michael Manga for helpful suggestions.

References

Bascle, B. J., L. D. Nixon, and K. M. Ross, Atlas of Gulf of Mexico gas and oil sancs [CD-ROM], *OCS Rep. MMS 2001-86*, Mineral Manage. Serv., New Orleans, La., 2001.

Booth, J. S., M. M. Rowe, and K. M. Fischer, Offshore gas hydrate sample database, *Open-File Rep. 96-272*, pp. 1–17, U.S. Geol. Surv., Reston, Va., 1996.

Brooks, J. M., M. C. Kennicutt II, R. R. Fay, T. J. McDonald, and R. Sassen, Thermogenic gas hydrates in the Gulf of Mexico, *Science*, *225*, 409–411, 1984.

Brooks, J. M., H. B. Cox, W. R. Bryant, M. C. Kennicutt II, R. G. Mann, and T. J. McDonald, Association of gas hydrates and oil seepage in the Gulf of Mexico, *Org. Geochem.*, *10*, 221–234, 1986.

Clennell, M. B., M. Hoveland, J. S. Booth, P. Henry, and W. J. Winters, Formation of natural gas hydrates in marine sediments, 1, Conceptual model of gas hydrate growth conditioned by host sediment properties, *J. Geophys. Res.*, *104*, 22,985–23,003, 1999.

Clennell, M. B., H. Pierre, M. Hovlane, J. S. Booth, W. Winters, and M. Thomas, Formation of natural gas hydrates in marine sediments: Gas hydrate growth and stability conditioned by host sediment properties, *Ann. N. Y. Acad. Sci.*, *912*, 887–896, 2000.

Collett, T. S., Natural-gas hydrates of the Prudhoe Bay and Kuparuk river area, North Slope, Alaska, *AAPG Bull.*, *77*(5), 793–812, 1993.

Collett, T. S., Gas hydrate resources of the US, in *National Assessment of U.S. Oil and Gas Resources* [CD-ROM], *USGS Digital Data Ser.*, vol. 30, edited by D. L. Gauter et al., U.S. Geol. Soc., Denver, Colo., 1995.

Collett, T. S., and V. A. Kuuskraa, Hydrates contain vast store of world gas resources, *Oil Gas J.*, *96*, 90–95, 1998.

Collett, T. S., and M. W. Lee, Reservoir characterization of marine and permafrost associated gas hydrate accumulations with downhole well logs, *Ann. N. Y. Acad. Sci.*, *912*, 51–64, 2000.

Cook, D., and P. D'Onfro, Jolliet Field thrust structure and stratigraphy, Green Canyon Block 184, offshore Louisiana, *Trans. Gulf Coast Assoc. Geol. Soc.*, *41*, 100–121, 1991.

Egeberg, P. K., and G. R. Dickens, Thermodynamic and pore water halogen constraints on gas hydrate distribution at ODP Site 997 (Blake Ridge), *Chem. Geol.*, *153*(1–4), 53–79, 1999.

Fu, B., and P. Aharon, Sources of hydrocarbon-rich fluids advecting on the seafloor in the northern Gulf of Mexico, *AAPG Bull.*, *82*(9), 1781, 1998.

Ginsburg, G. D., and V. A. Soloviev, Methane migration within the submarine gas-hydrate stability zone under deep-water conditions, *Mar. Geol.*, *137*, 49–57, 1997.

Ginsburg, G. D., and V. A. Soloviev, *Submarine Gas Hydrates*, 216 pp., VNIOkeangeologia, St. Petersburg, 1998.

Helgerud, M. B., J. Dvorkin, and A. Nur, Rock physics characterization for gas hydrate reservoirs Elastic properties, *Ann. N. Y. Acad. Sci.*, *912*, 116–125, 2000.

Kennicutt, M. C. II, J. M. Brooks, R. R. Bidigare, R. R. Fay, T. L. Wade, and T. J. MacDonald, Vent type taxa in a hydrocarbon seep region on the Louisiana slope, *Nature*, *317*, 351–353, 1985.

Kennicutt, M. C. II, J. M. Brooks, and G. J. Denoux, Leakage of deep, reservoired petroleum to the near surface of the Gulf of Mexico continental slope, *Mar. Chem.*, *24*, 39–59, 1988.

Kornacki, A. S., J. W. Kendrick, and J. L. Berry, Impact of oil and gas vents and slicks on petroleum exploration in the deepwater Gulf of Mexico, *Geo-Mar. Lett.*, *14*, 160–169, 1994.

Kvenvolden, K. A., A review of the geochemistry of methane in natural gas hydrate, *Org. Geochem.*, *23*, 997–1008, 1995.

Kvenvolden, K. A., A primer on the geological occurrence of gas hydrate, in *Gas Hydrates: Relevance to World Margin Stability and Climate Change*, edited by J. P. Henriet and J. Mienert, pp. 9–30, Geol. Soc., London, 1998.

MacDonald, I. R., N. L. Guinasso, R. Sassen, J. M. Brooks, L. Lee, and K. T. Scott, Gas hydrate that breaches the sea floor on the continental slope of the Gulf of Mexico, *Geology*, *22*, 699–702, 1994.

MacDonald, I. R., D. B. Buthman, W. W. Sager, M. B. Peccini, and N. L. Guinasso, Pulsed oil discharge from a mud volcano, *Geology*, *28*, 907–910, 2000.

Melnikov, V., and A. Nesterov, Modeling of gas hydrates formation in porous media, in *Second International Conference on Natural Gas Hydrates*, France, pp. 541–548, Assoc. PROGEP, Toulouse, France, 1996.

Miles, P. R., Potential distribution of methane hydrate beneath the European continental margins, *Geophys. Res. Lett.*, *22*(23), 3179–3182, 1995.

Milkov, A. V., and R. Sassen, Thickness of the gas hydrate stability zone, Gulf of Mexico continental slope, *Mar. Pet. Geol.*, *17*, 981–991, 2000.

Milkov, A. V., and R. Sassen, Estimate of gas hydrate resource, northwestern Gulf of Mexico continental slope, *Mar. Geol.*, *179*, 71–83, 2001.

Milkov, A. V., R. Sassen, I. Norikova, and E. Mikhailov, Gas hydrates at minimum stability water depths in the Gulf of Mexico: Significance to geohazard assessment, *Trans. Gulf Coast Assoc. Geol. Soc.*, *50*, 217–224, 2000.

Rempel, A. W., and B. A. Buffett, Formation and accumulation of gas hydrate in porous media, *J. Geophys. Res.*, *102*, 10,151–10,164, 1997.

Roberts, H. H., Surficial geology of the middle and upper continental slope, northern Gulf of Mexico; the important role of episodic fluid venting, *AAPG Bull.*, *80*(9), 1511, 1996.

Roberts, H. H., Fluid and gas expulsion on the Northern Gulf of Mexico continental slope: Mud-prone to mineral-prone responses, in *Natural Gas Hydrates: Occurrence, Distribution, and Detection*, edited by C. K. Paull and W. P. Dillon, pp. 145–161, AGU, Washington, D. C., 2001.

Roberts, H. H., and P. Aharon, Hydrocarbon-derived carbonate buildups of the Northern Gulf-of-Mexico continental-slope - a review of submersible investigations, *Geo-Mar. Lett.*, *14*, 135–148, 1994.

Roberts, H. H., and R. S. Carney, Evidence of episodic fluid, gas, and sediment venting on the northern Gulf of Mexico continental slope, *Econ. Geol.*, *92*(7–8), 863–879, 1997.

Ruppel, C., Anomalously cold temperatures observed and the base of the gas hydrate stability zone on the U.S. Atlantic passive margin, *Geology*, *25*, 699–702, 1997.

Sassen, R., and I. R. MacDonald, Evidence of structure H hydrate, Gulf of Mexico continental slope, *Org. Geochem.*, *22*, 1029–1032, 1994.

Sassen, R., and I. R. MacDonald, Hydrocarbons of experimental and natural gas hydrates, Gulf of Mexico continental slope, *Org. Geochem.*, *26*, 289–293, 1997.

Sassen, R., J. M. Brooks, and M. C. Kennicutt, How oil seeps, discoveries relate in deepwater Gulf of Mexico, *Oil Gas J.*, *91*, 64–69, 1993.

Sassen, R., I. R. MacDonald, N. L. Guinasso, S. Joyce, A. G. Requejo, S. T. Sweet, J. Alcala-Herrera, D. DeFreitas, and D. R. Schink, Bacterial methane oxidation in sea-floor gas hydrate: Significance to life in extreme environments, *Geology*, *26*, 851–854, 1998.

Sassen, R., S. Joyce, S. T. Sweet, D. A. DeFreitas, A. V. Milkov, and I. R. MacDonald, Thermogenic gas hydrates and hydrocarbon gases in complex chemosynthetic communities, Gulf of Mexico continental slope, *Org. Geochem.*, *30*, 485–497, 1999a.

Sassen, R., S. T. Sweet, A. V. Milkov, D. A. DeFreitas, G. G. Salata, and E. C. McDade, Geology and geochemistry of gas hydrates, Central Gulf of Mexico continental slope, *Gulf Coast Assoc. Geol. Soc., Trans.*, *XLIX*, 462–468, 1999b.

Sassen, R., S. T. Sweet, D. A. DeFreitas, and A. V. Milkov, Exclusion of 2-methylbutane (isopentane) during crystallization of structure II gas hydrate in sea-floor sediment, Gulf of Mexico, *Org. Geochem.*, *31*, 1257–1262, 2000.

Sassen, R., S. L. Losh, L. Cathles, H. H. Roberts, J. K. Whelan, A. V. Milkov, S. T. Sweet, and D. A. DeFreitas, Massive vein-filling gas hydrate: Relation to ongoing gas migration from the deep subsurface in the Gulf of Mexico, *Mar. Petrol. Geol.*, *18*, 551–560, 2001a.

Sassen, R., S. T. Sweet, A. V. Milkov, D. A. DeFreitas, and M. C. Kennicutt, Stability of thermogenic gas hydrate in the Gulf of Mexico: Constraints on models of climate change, in *Natural Gas Hydrates: Occurrence, Distribution, and Detection*, edited by C. K. Paull and W. P. Dillon, pp. 131–143, AGU, Washington, D. C., 2001b.

Sassen, R., S. T. Sweet, A. V. Milkov, D. A. DeFreitas, and M. C. Kennicutt, Thermogenic vent gas and gas hydrate in the Gulf Of Mexico Slope: Is gas hydrate decomposition significant?, *Geology*, *29*, 107–110, 2001c.

Sloan, E. D., *Clathrate Hydrates of Natural Gases*, 2nd ed., 628 pp., Marcel Dekker, New York, 1998.

Wenger, L. M., L. R. Goodoff, O. P. Gross, S. C. Harrison, and K. C. Hood, Northern Gulf of Mexico: An integrated approach to source, maturation, and migration, paper presented at Geological Aspects of Petroleum System, Proceedings, First Joint American Association of Petroleum Geologists/Association Mexican de Geologos Petroleos Research Conference, Mexico City, 1994.

Xu, W., and C. Ruppel, Predicting the occurrence, distribution, and evolution of methane gas hydrate in porous marine sediments, *J. Geophys. Res.*, *104*, 5081–5095, 1999.

L. M. Cathles III, Department of Geological Sciences, Cornell University, Ithaca, NY 14853-1504, USA. (cathles@geology.cornell.edu)

D. F. Chen, Guangzhou Institute of Geochemistry, Chinese Academy of Sciences, Guangzhou, China.